BBA - Biomembranes 1866 (2024) 184334

Contents lists available at ScienceDirect

BBA - Biomembranes

journal homepage: www.elsevier.com/locate/bbamem

Cholesterol drives enantiospecific effects of ibuprofen in biomimetic membranes

Alexa Guglielmelli [a,b,1], Caterina M. Tone [c,b,1], Eleonora Ragozzino [d], Federica Ciuchi [b], Rosa Bartucci [d,*]

[a] Department of Physics, NLHT Lab, University of Calabria, 87036 Rende, Italy
[b] CNR NANOTEC c/o Department of Physics, University of Calabria, 87036 Rende, Italy
[c] Department of Physics, Molecular Physics Group, University of Calabria, 87036 Rende, Italy
[d] Department of Physics, Molecular Biophysics Lab, University of Calabria, 87036 Rende, Italy

ARTICLE INFO

Keywords:
DPPC/cholesterol bilayers
Supported DPPC/cholesterol monolayers
Ibuprofen enantiomers
CD
ESR
AFM

ABSTRACT

The interaction between chiral drugs and biomimetic membranes is of interest in biophysical research and biotechnological applications. There is a belief that the membrane composition, particularly the presence of cholesterol, could play a pivotal role in determining enantiospecific effects of pharmaceuticals. Our study explores this topic focusing on the interaction of ibuprofen enantiomers (S- and R-IBP) with cholesterol-containing model membranes. The effects of S- and R-IBP at 20 mol% on bilayer mixtures of dipalmitoylphosphatidylcholine (DPPC) with 0, 10, 20 and 50 mol% cholesterol were investigated using circular dichroism and spin-label electron spin resonance. Morphological changes due to IBP enantiomers were studied with atomic force microscopy on supported cholesterol-containing DPPC monolayers. The results reveal that IBP isoforms significantly and equally interact with pure DPPC lipid assemblies. Cholesterol content, besides modifying the structure and the morphology of the membranes, triggers the drug enantioselectivity at 10 and 20 mol%, with the enantiomers differently adsorbing on membranes and perturbing them. The spectroscopic and the microscopic data indicate that IBP stereospecificity is markedly reduced at equimolar content of Chol mixed with DPPC. This study provides new insights into the role of cholesterol in modulating enantiospecific effects of IBP in lipid membranes.

1. Introduction

The lipid bilayer component, in addition to the protein component, is fundamental in regulating the structure/function relationship in cell membranes. The bilayer sector represents a template where key molecular processes take place and, in many circumstances, it is the target of many exogenous and endogenous ligands. Over the years, models of cell membranes, especially lipid bilayers, and their interactions with drugs, have received considerable attention in biomedical and biotechnological fields, such as drugs design and delivery, drugs cellular uptake, and understanding of their side effects [1–3]. Even more interesting is the possibility of chiral recognition of drugs and compounds on lipid bilayers [4–9], which paves the way to selective sensing and other relevant applications [10,11].

A number of studies have indicated the membrane composition as an important factor in determining the possibility of enantiomeric selectivity of chiral compounds in membranes [5,8,12–16]. In fact, it has been evidenced that neutral and anionic lipid bilayers are differently sensitive to amino acids chirality [16]. Moreover, the heterogeneity, i.e., presence of nano- or meso-domains [14,15], as well as the inclusion of cholesterol [5,8] in membranes could induce chiral separations.

In this study, our aim is to explore the interaction between lipid membrane and chiral drugs, with a specific focus on understanding how the membrane composition influences the enantiorecognition of ibuprofen (IBP), one of the most used non-steroidal anti-inflammatory drugs worldwide. IBP exists as a pair of enantiomers: S-IBP and R-IBP. The biological effects of the enantiomers differ significantly: S-IBP is the active form responsible for the desired therapeutic effects, while R-IBP is considered pharmacologically inactive [17]. We varied the membrane composition by considering lipid assemblies containing cholesterol. Specifically, as membrane model systems, we used both fully hydrated bilayers and supported monolayers composed of either

* Corresponding author.
E-mail address: rosa.bartucci@fis.unical.it (R. Bartucci).
[1] These authors contributed equally.

https://doi.org/10.1016/j.bbamem.2024.184334
Received 21 February 2024; Received in revised form 3 April 2024; Accepted 11 May 2024
Available online 12 May 2024

dipalmitoylphosphatidylcholine (DPPC) or binary mixtures of DPPC and cholesterol (Chol). The zwitterionic DPPC lipids are abundant in cell membranes and Chol is a steroid that is a major integral component of eukaryotic mammalian cells [18,19]. While the behavior of IBP in model membranes (both single lipid species and Chol/lipid mixtures) is discussed in the literature [20–30], not many are the studies about interaction of IBP enantiomers with cholesterol-containing membranes [15]. To get more insight into the interplay between IBP enantiomers and cholesterol in lipid membranes, we focused on pure DPPC and on mixtures of DPPC with 10, 20 or 50 mol% of Chol. For each membrane composition, we present results in the absence and in the presence of 20 mol% of either R- or S-IBP. The binary DPPC/Chol mixtures serve as intriguing platforms for probing the interaction of IBP isomers with lipid membranes, as they form a variety of structural phases, which include the solid-ordered, S_o, the liquid-disordered, L_d, and the liquid-ordered, L_o, phases as well as the (S_o + L_o) and (L_d + L_o) phase coexistence (see, e.g., [31,32] and references therein). The content of 20 mol% of IBP was chosen as it alters the molecular properties of lipid membranes without changing their phase state [25–27]. The study is carried out by using jointly spectroscopic techniques and, for the first time, microscopic methods. The absorption of the ibuprofen isoforms on the fully hydrated bilayers is assessed by circular dichroism (CD) exploiting the characteristic signal of IBP at around 227 nm [33]. The enantio-influence of IBP on the lipid order and dynamics as a function of temperature is investigated by electron spin resonance (ESR) spectroscopy using TEMPO-Stearate as polarhead spin-labelled lipids and phosphatidylcholine spin-labelled at C4 (4-PCSL) and C14 (14-PCSL) positions along the hydrocarbon chains. The morphological changes arising from the addition of S- or R-IBP in pure DPPC matrices and in DPPC/Chol binary mixtures were studied by atomic force microscopy (AFM) on mica supported monolayer lipid films.

2. Materials and methods

2.1. Materials

The synthetic lipid 1,2-dipalmitoyl-sn-glycero-3-phosphocholine (DPPC) was from Avanti Polar Lipids (Birmingham, AL, USA). S-ibuprofen (S(+)-4-Isobutyl-α-methylphenylacetic acid) was purchased from Sigma-Aldrich (St. Louis, MO, USA), whereas R-ibuprofen (R(−)-4-Isobutyl-α-methylphenylacetic acid) was from Cayman Chemical (Ann Arbor, MI, USA). The purity of the drugs was ≥98 %. Cholesterol (5-colestene-3β-olo, from porcine liver, purity ≥98 %) and the polarhead-labelled lipid, 2,2,6,6-tetramethyl-piperidin-1-oxyl-4-yl octadecanoate (TEMPO-Stearate) were from Sigma-Aldrich. The chain-labelled phosphatidylcholine, 1-acyl-2-(*n*-doxyl) stearoyl-*sn*-glycero-3-phosphocholine) with $n = 4$ (4-PCSL) was synthesized according to [34], whereas that with $n = 14$ (14-PCSL) was obtained from Avanti Polar Lipids. Dulbecco's phosphate-buffered saline solution (10 mM, pH 7.4) was from Sigma-Aldrich and Milli-Q grade deionized water from Millipore. All the analytical grade chemicals were used as provided, without any further purification.

2.2. Sample preparation

The model systems of cell membranes used in this study are hand shaken multilamellar lipid dispersions for CD and ESR measurements, and Langmuir films supported on mica for AFM measurements. Multilamellar lipid dispersions, also known as liposomes, and hereafter referred to as lipid bilayers, are prepared according to the thin film hydration method [35] and as it is reported everywhere [36,37]. Pure DPPC or mixtures of DPPC with Chol at 10, 20, and 50 mol%, either in the absence or in the presence of S- and R-IBP at 20 mol% of the total lipid concentration, were codissolved in chloroform/methanol (2:1 v/v). The solvent was first evaporated under a gentle nitrogen gas stream and then under vacuum overnight, to ensure proper solvent removal. The dry films were dispersed in buffer by heating at 50 °C, i.e., above the bilayers main phase transition temperature of any composition, and occasionally vortexing until an opalescent bilayer suspension was obtained. Samples were incubated for 24 h before measuring.

Langmuir films were prepared in a clean room at room temperature by using a 622 NIMA Langmuir-Pockels trough, starting from chloroform solution of the pure materials and their mixtures, in the same molar percentage used for bilayer samples. Freshly cleaved mica was immersed in the water subphase (Milli-Q grade deionized water) before spreading phospholipid solutions and the monolayer pressure was kept constant at 20 mN/m during the deposition. This procedure allows to obtain a supported monolayer in which the polar groups are in contact with the mica surface and the hydrophobic portion is exposed to the air.

2.3. Circular dichroism

For CD measurements, cholesterol-containing DPPC bilayers in the absence and in the presence of S- or R-IBP were prepared at the final lipid concentration of 1.36 mM. CD spectra of S- or R-IBP in aqueous solutions or incorporated in cholesterol-containing DPPC bilayers were recorded at 25 °C with a Jasco J-1700 spectropolarimeter in the range of 190–260 nm under constant gaseous N_2 supply by using a 1 mm path length quartz cuvette. The spectra were measured with a scan speed of 50 nm/min, a bandwidth of 1.0 nm, a resolution of 0.2 nm, and a PMT voltage of below 600 V. Each spectrum is an average of at least 5 scans. All spectra were background-subtracted.

CD spectra were used to evaluate the adsorbed concentration of S- or R-IBP on lipid membranes (C_{ads}) by using the following equation [15]:

$$C_{ads} = C_{ini} - C_{sup} \tag{1}$$

where C_{ini} is the initial concentration of S- or R-IBP, i.e., that used in sample preparation corresponding to 20 mol% of total lipid concentration, and C_{sup} is the IBP concentration in the supernatant of the aqueous lipid bilayer dispersions. C_{sup} was derived by using the CD version of the Beer-Lambert law for absorbance [38]:

$$CD = \Delta A\ (absorbance\ units) = A_L - A_R = (\Delta\varepsilon)\ C\ l \tag{2}$$

Here, *CD* is the intensity of the circular dichroic signal, A_L and A_R are the absorptions of left- and right-circularly polarized light, l is the optical path in cm, C is the IBP concentration in M, and Δε is the differential extinction coefficient in M^{-1} cm^{-1}. To determine Δε, CD spectra of IBP were recorded at increasing drug concentration (see Fig. S1a). The data were then used to set a calibration curve, i.e., a linear plot of the intensity of the CD signal at 227 nm versus IBP concentration (Fig. S1b), from which the slope, i.e., Δε, has been deduced. This Δε value was finally used to estimate the IBP concentration in the supernatant, C_{sup}, of the various cholesterol-containing DPPC bilayers according to Eq. (2).

The separation parameter, $S_{R/S}$, which provides a measure of the degree of enantiospecificity, was calculated by the following equation [15]:

$$S_{R/S} = \frac{C_{ads}^{R-IBP}}{C_{ads}^{S-IBP}} \tag{3}$$

where C_{ads}^{S-IBP} and C_{ads}^{R-IBP} are the concentration of S- and R- form of IBP adsorbed on the lipid bilayers, respectively.

2.4. Spin-label electron spin resonance

Samples for ESR measurements were fully hydrated lipid bilayers at the final lipid concentration of 50 mM obtained by co-dissolving the lipids with 0.5 mol% of spin-labels (either TEMPO-stearate or *n*- PCSL). Hydrated samples were centrifuged at 3000 rpm for 20 min at room temperature and the excess aqueous supernatant was removed. The pellets were loaded in glass capillaries (ID 1 mm), which were then

inserted in a standard 4-mm ESR quartz tube containing silicone oil to avoid thermal gradients. ESR spectra were acquired on a ELEXSYS E580 spectrometer (Bruker, Karlsruhe, Germany) operating at 9 GHz with 100-kHz field modulation and equipped with a Bruker ER 4111 VT temperature controller and a Bruker ER 4201 TE_{102} rectangular cavity in the center of which was accommodated the sample tube. ESR spectra were recorded on heating, well below saturation at a microwave power of 10 mW with 1–1.5 G_{p-p} magnetic field modulation amplitude. Multiple scans were accumulated to increase the signal-to-noise ratio.

In any given CD or ESR experiment, two or three independent measurements were executed. Representative spectra are shown in the figures, and the data points and parameters are mean ± standard error, where the standard error is the semidispersion of the data.

2.5. Atomic force microscopy

Topographic images of Langmuir thin films were acquired using a Bruker Multimode 8 AFM equipped with a Nanoscope V controller. Measurements were carried out in Peak Force mode at room temperature, at least one day after the monolayer deposition, to allow complete water evaporation. Silicon cantilevers (model RTESPA-300, Burker) with 10 nm tip radius and 42 N/m elastic constant were used to collect the topographic images, with a scan rate of 0.7 Hz. To analyze the images and evaluate the topographic features, we used both the freely distributed analysis software Gwyddion (GNU General Public License) [39] and the Nanoscope Analysis software (Bruker). In any given experiment, two independent measurements were executed to test their reproducibility.

3. Results and discussion

3.1. Circular Dichroism: enantiospecific adsorption of IBP on cholesterol-containing lipid bilayers

Fig. 1a shows the CD signals of IBP chiral forms in aqueous solutions and in the different lipid membranes.

As expected, the CD signals of S- and R-IBP are opposite, nearly mirror images, and in the range of 200–260 nm with characteristic ellipticity maxima/minima at about 227 nm [33]. Notable changes are seen in the intensity of dichroic ibuprofen signal when the drug is incubated with the lipid membranes. Particularly, a membrane composition-dependent decrease is detected with respect to the IBP reference signal obtained at 0.270 mM (i. e., [IBP] = 20 mol% lipid concentration).

The observed changes in the ibuprofen CD intensity in Fig. 1a were found to be correlated with the adsorbed drug concentration. Specifically, as it can be observed in Fig. 1b, when the percentage of cholesterol in the lipid mixtures increases, there is a significant decrease in drug adsorption. Indeed, the percentage of adsorbed IBP decreases from about 50 % in pure DPPC to about 40 % and to 15–20 % in mixtures of DPPC with 10 or 20 mol% of Chol, respectively. The percentage of C_{ads} drops to about 10 % in DPPC with equimolar content of cholesterol. These values are comparable to those reported for the adsorption of IBP on zwitterionic phosphocholine membranes [15]. Moreover, it can be observed that while no enantioselectivity occurs on DPPC, as the adsorption percentage is the same for both IBP enantiomers (see, Fig. 1b), the interaction becomes more enantiospecific with the presence of cholesterol, with the R-form being slightly more adsorbed than S-form. This is further supported by the separation parameter $S_{R/S}$, (Fig. 1b, red curve) which increased from 1 for DPPC to about 1.5 for DPPC+20 mol% cholesterol to 1.75 for DPPC+50 mol% cholesterol. It is worth underlining that the value of C_{ads} of IBP in DPPC+50 mol% Chol is very low, around 10 %, thus making its ability to distinguish the two chiral forms, although present, negligible.

The CD results indicate that the presence of cholesterol decreases the adsorption of IBP on DPPC bilayers and, at the same time, triggers the enantiospecificity of the IBP-membrane interaction. The results align with prior studies. In fact, a decreased adsorption of Amphotericin B has been reported on vesicles of phosphatidylcholines in the presence of cholesterol, and this has been ascribed to changes of the membrane characteristics induced by the steroid [40]. Moreover, enantiospecific effects of chiral molecules are observed when cholesterol is mixed with lipids in membranes [5,8]. Chiral selective adsorption of IBP was found to occur on cholesterol-containing ternary lipid membranes [15].

3.2. Spin-label ESR

To investigate the effects of IBP isoforms on cholesterol-containing DPPC membranes in different physical states and membrane regions, temperature-dependent ESR measurements were performed by using TEMPO-Stearate (i.e., a polarhead-labelled lipid), 4-, and 14-PCSL (i.e., two chain-labelled lipids that probe, respectively, the first and the terminal chain segments of the hydrocarbon zone of the membranes). Results on the effects of IBP isoforms are presented first on pure DPPC bilayers and then on mixtures of DPPC with Chol.

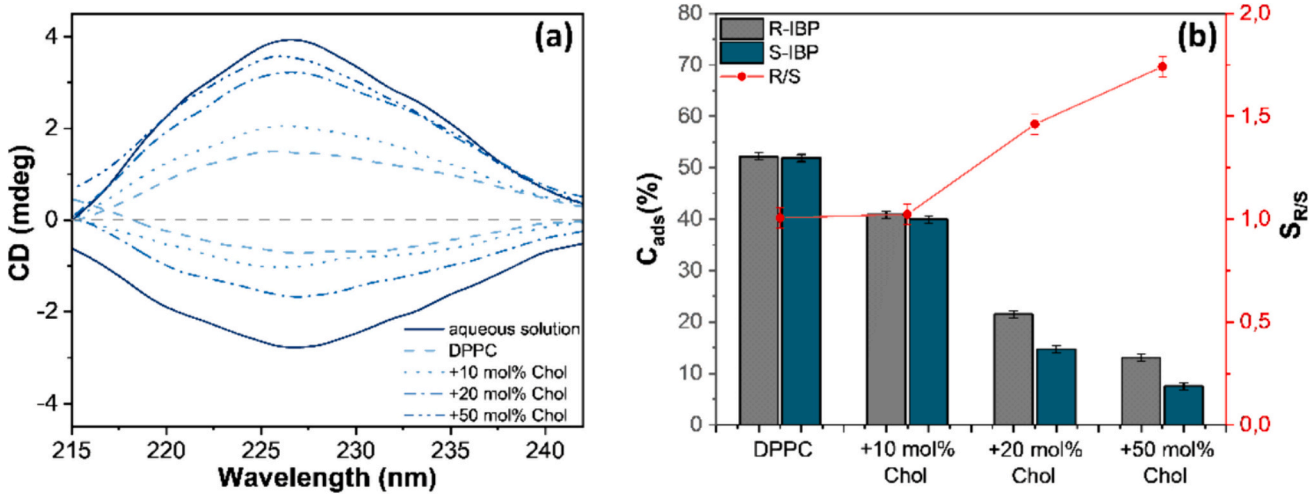

Fig. 1. (a) Circular dichroism spectra of S-Ibuprofen (positive signals) and R-Ibuprofen (negative signals) in aqueous solutions and in cholesterol-containing DPPC bilayers. In any sample, the Ibuprofen concentration is 0.270 mM, i.e., 20 mol% of total lipid concentration. (b) (left vertical axis) Percentage of adsorbed concentration of Ibuprofen isomers, C_{ads}, and (right vertical axis) separation parameter, $S_{R/S}$, as a function of lipid bilayers composition.

3.2.1. Single-component lipid membrane: the IBP chiral forms affect similarly DPPC bilayers

In Fig. 2 are shown the ESR spectra of TEMPO-Stearate (left panel), 4-PCSL (central panel) and 14-PCSL (right panel) in bilayers of pure DPPC and DPPC doped with S-IBP at 20, 35 and 45 °C. The spin-label spectra for DPPC doped with R-IBP are not shown as they are nearly superimposable to those obtained with S-IBP.

In any sample, the spectral anisotropy decreases on increasing the temperature but at different extents. Moreover, compared to pure DPPC, for each type of label, the spectral anisotropy is differently affected by IBP at the various temperatures.

For the polarhead-labelled TEMPO-Stearate, the spectra can be readily analyzed by evaluating the peak-to-peak linewidth of the low-field first resonance line, ΔH^L_{p-p} (see Fig. 2, left panel). The parameter reflects the polarhead packing and dynamics of the lipid samples: the greater ΔH^L_{p-p}, the more densely packed the polarhead regions and the lower the spin-label mobility [41,42]. Some remarkable features can be observed from the temperature dependence of ΔH^L_{p-p} in the left panel of Fig. 3. In any sample, the linewidth reduces with increasing the temperature, as a result of the temperature-induced decrease of the spectral anisotropy. Moreover, the IBP molecules, upon interacting with DPPC, reduce ΔH^L_{p-p} at 20 and at 35 °C, whereas they have no effect at 45 °C. In addition, the two enantiomeric IBP forms affect at the same extent ΔH^L_{p-p} at any temperature.

The ESR findings of TEMPO-Stearate clearly indicate that the drug loosens the molecular DPPC polarhead packing without enantiospecificity for temperatures through the solid-ordered gel phase, S_0.

By comparing the spectra of 4-PCSL in pure DPPC and in DPPC/S-IBP reported in the central panel of Fig. 2, it can be seen that the addition of the drug reduces the spectral anisotropy, slightly at 20 and 45 °C and markedly at 35 °C. All the ESR spectra of 4-PCSL can be analyzed in terms of the outer hyperfine splitting, $2A_{max}$, i.e., the separation between the outermost resonances (see Fig. 2, central panel). This parameter is an empirical measure of the lipid chain order and dynamics: the larger the anisotropy, the greater the $2A_{max}$ value and the higher the order and the motional restriction of the lipid chain [41,42]. Plots of $2A_{max}$ versus temperature are also used to detect the lipid phase transitions, as discontinuities occur at temperatures corresponding to the thermotropic phase transitions of the lipid bilayers [43]. To follow the thermal behavior of DPPC, ESR spectra of 4-PCSL were acquired at several different temperatures.

The temperature dependences of $2A_{max}$ for 4-PCSL in DPPC and in IBP-containing DPPC bilayers are given in the central panel of Fig. 3. The plots indicate that, without stereospecificity, both IBP forms leave unaffected the packing and the rotational mobility of the first acyl chain segments of DPPC in the gel state, downshift the $S_o \rightarrow L_d$ bilayer main phase transition temperature, T_m, and slightly increase the segmental chain disorder and rotational mobility in the fluid state.

The spectra of 14-PCSL in any DPPC sample and at any temperature (Fig. 2, right panel) display a lower anisotropy compared to the corresponding spectra of 4-PCSL. This is expected when the nitroxide moiety probes the inner hydrocarbon bilayer regions that is more disorder with respect to the first acyl chain segments probed by 4-PCSL. For DPPC/14-PCSL sample in Fig. 2, the extent of spectral anisotropy decreases rapidly on increasing the temperature from the solid-ordered to the liquid-disordered phase. At the highest temperature, the spectra, because of the high degree of motional narrowing, resemble almost isotropic triplets with differential line broadening, as it normally occurs for a spin-labelled lipid close at the terminal methyl end such as 14-PCSL [43]. From the spectra of 14-PCSL in right panel of Fig. 2 can be seen that the addition of S-IBP in DPPC bilayers reduces the spectral anisotropy at the lowest temperature (i.e., 20 °C), whereas it leaves almost unaffected the spectral lineshape at the other temperatures both in the gel (i.e., 35 °C) and in the fluid state (i.e., 45 °C). Quantitatively, the spectra of 14-PCSL in DPPC samples can be compared by evaluating the difference $\Delta A = 2A_{max}\text{-}2A_{min}$ between the outer, $2A_{max}$, and the inner, $2A_{min}$, hyperfine separations (see Fig. 2, right panel). ΔA is a spectral parameter useful to discuss the bilayer order and dynamics when lipids labelled at the terminal chain segments such as 14-PCSL are used: the lower the anisotropy, the lower ΔA and the higher chain disorder and mobility [42]. The temperature dependences of ΔA for 14-PCSL in pure DPPC and in DPPC + IBP enantiomers in the right panel of Fig. 3 indicate that IBP isoforms without stereospecificity influence the deep interior of DPPC bilayers at the lowest temperature by loosening the chain packing and increasing the segmental chain flexibility.

On the whole, the spin-label ESR results clearly indicate that the IBP enantiomers equally, i.e., without enantiospecificity, reduce the molecular packing of the polarhead as well as the conformational order of the hydrocarbon region of DPPC mainly for temperatures through the solid-ordered gel phase, and lower the main phase transition temperature. These ESR findings are in agreement with previous literature data obtained with racemic-IBP in phosphatidylcholine bilayers. In fact, a down-shift of T_m is reported from calorimetric and spectroscopic results in DMPC/IBP complexes [20,21,25,27]. Small angle neutron scattering and neutron spin echo techniques revealed that IBP makes the membrane thinner, more disordered, and softer; these effects were dependent on the membrane physical state, being more pronounced in the gel state [28]. Enhanced mobility of the lipid headgroups and some degree of disordering in the membrane were imposed by the addition of IBP in POPC as shown by ^2H and ^{31}P NMR data [29]. Moreover, our ESR findings, in close accordance with CD analyses, do not evidence any differentiation between S- and R-enantiomers in the interaction with DPPC bilayers. Various liposomes with different phase transition temperatures, such as DOPC ($T_m \approx -22$ °C), DLPC ($T_m \approx 0$ °C), DMPC ($T_m \approx 24$ °C), and DPPC ($T_m \approx 41$ °C) displayed very low or even null (in the case of DPPC) chiral recognition toward IBP [15].

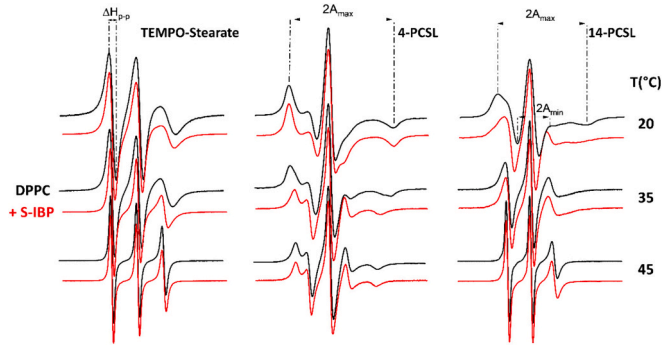

Fig. 2. ESR spectra at 20, 35, and 45 °C of TEMPO-stearate (left panel), 4-PCSL (central panel), and 14-PCSL (right panel) in DPPC (upper spectra, black lines) and DPPC+20 mol% S-IBP (lower spectra, red lines). Total spectral width = 100 G.

3.2.2. DPPC/Chol binary mixtures: cholesterol modulates the enantioselective influence of IBP on DPPC bilayers

Before studying the influence of IBP enantiomers on cholesterol-containing DPPC bilayers, we present spin-label ESR results on IBP-free DPPC/Chol mixtures, which will then be used as references.

The spectra of TEMPO-stearate, 4- and 14-PCSL in DPPC with 10, 20, and 50 mol% Chol at 20, 35, and 50 °C are reported in the Fig. S2, whereas the temperature dependences of ΔH^L_{p-p} for TEMPO-Stearate, $2A_{max}$ for 4-PCSL, and ΔA for 14-PCSL in the same samples are reported in the Fig. 4. All the cholesterol-induced effects on DPPC can be readily discussed from the plots in Fig. 4.

For TEMPO-stearate, ΔH^L_{p-p} decreases with increasing temperature in any sample; the rate of decrease changes in the order: 10 mol% > 20 mol% ≈ DPPC >50 mol%, which is very limited. Moreover, with respect

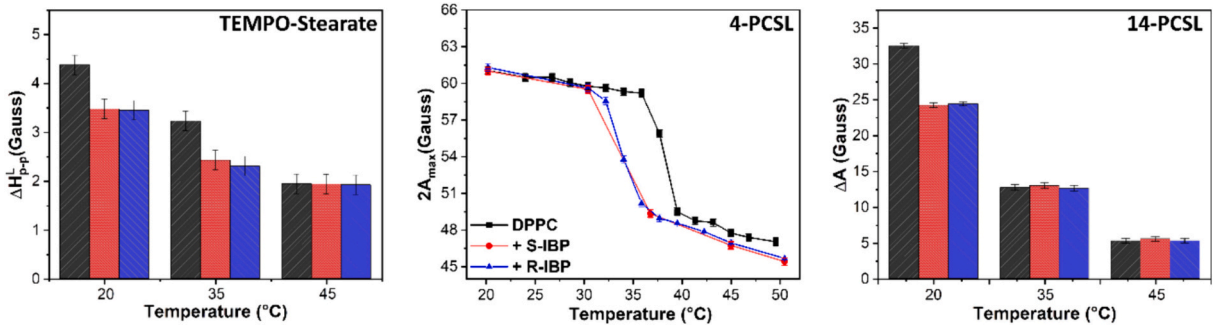

Fig. 3. Temperature dependence of ΔH^L_{p-p} of TEMPO-stearate, $2A_{max}$ of 4-PCSL, and ΔA of 14-PCSL in DPPC bilayers in the absence (black) and in the presence of 20 mol% of S-IBP (red) or R-IBP (blue).

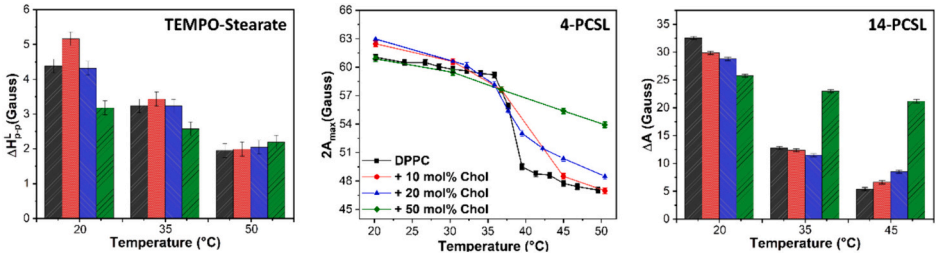

Fig. 4. Temperature dependence of ΔH^L_{p-p} of TEMPO-Stearate (left panel), $2A_{max}$ of 4-PCSL (central panel), and ΔA of 14-PCSL (right panel) in DPPC bilayers (black) and in mixtures of DPPC+10 mol% Chol (red), DPPC+20 mol% Chol (blue), DPPC+50 mol% Chol (green).

to pure DPPC, it can be observed that i) the addition of 10 mol% Chol notably increases ΔH^L_{p-p} at 20 °C and moderately at 35 °C; ii) the addition of 20 mol% does not produce noticeable effects; iii) the addition of 50 mol% markedly reduces ΔH^L_{p-p} at 20 and 35 °C; iv) negligible or very slight effects are recorded at 45 °C in any lipid mixture.

The concentration- and temperature-dependent influence of cholesterol on the molecular organization of the DPPC polar region, which is reflected in the plots of TEMPO-Stearate in Fig. 4, indicates an augmented packing at low Chol content (10 mol%) and low temperatures (more at 20 than at 35 °C). This effect reverses at 50 mol% Chol: a reduced polarhead packing density occurs at the lowest temperatures (20 and 35 °C) for the cholesterol-induced increase in the area per polarhead.

For 4-PCSL in mixtures of DPPC with 10 or 20 mol% of Chol, the plots of $2A_{max}$ versus temperature in Fig. 4 display the main phase transitions, as expected from the temperature-cholesterol content phase diagrams for DPPC/Chol mixtures ([31,32] and references therein). With respect to the $S_o \rightarrow L_d$ transition in DPPC, they are less cooperative and occur at almost the same temperature. Moreover, for DPPC+10 mol% Chol, $2A_{max}$-values are higher for temperatures $T < T_m$ and are unchanged for $T > T_m$. This indicates a cholesterol-induced augmented chain order and mobility restriction in the upper chain zone of DPPC bilayers. Similar perturbations are induced by 20 mol% cholesterol in the $S_o + L_o$ state (i.e., at the lowest temperatures, for $T < T_m$) but a stronger effect of spin-label immobilization and chain ordering is seen in the $L_d + L_o$ state (i.e., at the highest temperature, for $T > T_m$). A drastic influence in the temperature trend of $2A_{max}$(4-PCSL) is seen in DPPC+50 mol% cholesterol. In these samples in the L_o state, a slow progressive reduction of $2A_{max}$ from about 63 G to about 55 G is observed when the temperature passes from 20 °C to 50 °C without showing any phase transition.

For 14-PCSL, the rate of continuous reduction with temperature of ΔA in Fig. 4 changes in the order: DPPC > DPPC+10 mol% Chol > DPPC+20 mol% Chol ≫ DPPC+50 mol% Chol. In fact, between 20 °C and 45 °C, ΔA reduces from 32 G to 5 G in DPPC, from 30 G to 7 G in presence of 10 mol% Chol, from 29 G to 8 G at 20 mol% Chol, and only from 26 G to 21 G in the L_o phase formed at 50 mol% Chol. So that, in the deep hydrocarbon region of the bilayers, with respect to what occurs in pure DPPC, cholesterol at any content induces disorder at the lowest temperature and promotes packing at the highest temperature; the biggest effect being observed in the L_o phase. The homogeneous L_o phase formed by DPPC +50 mol% Chol is characterized by dense chain packing and restricted mobility through the 20–50 °C temperature range. Such effects are observed in any membrane region, in the polarhead, at the polar-apolar interface and at the bilayer midplane sampled by TEMPO-stearate, 4-PCSL and 14-PCSL, respectively. This dense packing is expected for lipid/cholesterol equimolar mixtures, particularly for membrane raft domains [44–46].

ESR measurements of polarhead-labelled (i.e., TEMPO-Stearate) and chain-labelled lipids (i.e., 4- and 14-PCSL) in cholesterol-containing membrane have been recorded as a function of temperature in presence of R- or S-IBP. The spectra recorded at 20 °C in the different lipid matrices are reported in the Fig. S3, whereas the plots of ΔH^L_{p-p}(Tempo-Stearate), $2A_{max}$(4-PCSL) and ΔA (14-PCSL) versus temperature are shown in the Fig. 5.

The ESR results in Fig. S3 and Fig. 5 indicate that the enantiomers differently affect the DPPC bilayers containing 10 and 20 mol% of cholesterol. In these matrices, S-and R-IBP at different extent i) loosen the molecular packing in the polarhead regions through the $S_o + L_o$ state (see the decrease of ΔH^L_{p-p} (TEMPO-Stearate)); ii) change the chain order and induce disordering at 20 mol% Chol in the upper segments of hydrocarbon chains through the whole temperature range (see the reduction of $2A_{max}$(4-PCSL)); iii) slightly disorder the bilayer midplanes at the lowest temperature (see data ΔA(14-PCSL)); iv) perturb the thermotropic phase behavior by downshifting the temperature of the $(S_o + L_o) \rightarrow (L_d + L_o)$ transitions and reducing their cooperativity. It is worth stressing that IBP isomers induce disorder in cholesterol-containing DPPC bilayers, as was seen in pure DPPC (see Figs. 2 and 3).

The results agree with i) the pronounced fluidizing effect of 10 mol% IBP in the presence of 15 mol% Chol in DPPC membranes at 25 °C [26], and ii) the molecular disordering of 10 mol% IBP in the presence of 20 mol% Chol in low-T_m POPC membranes [29], and with iii) data obtained by molecular dynamics simulations about the influence of chol (0, 25

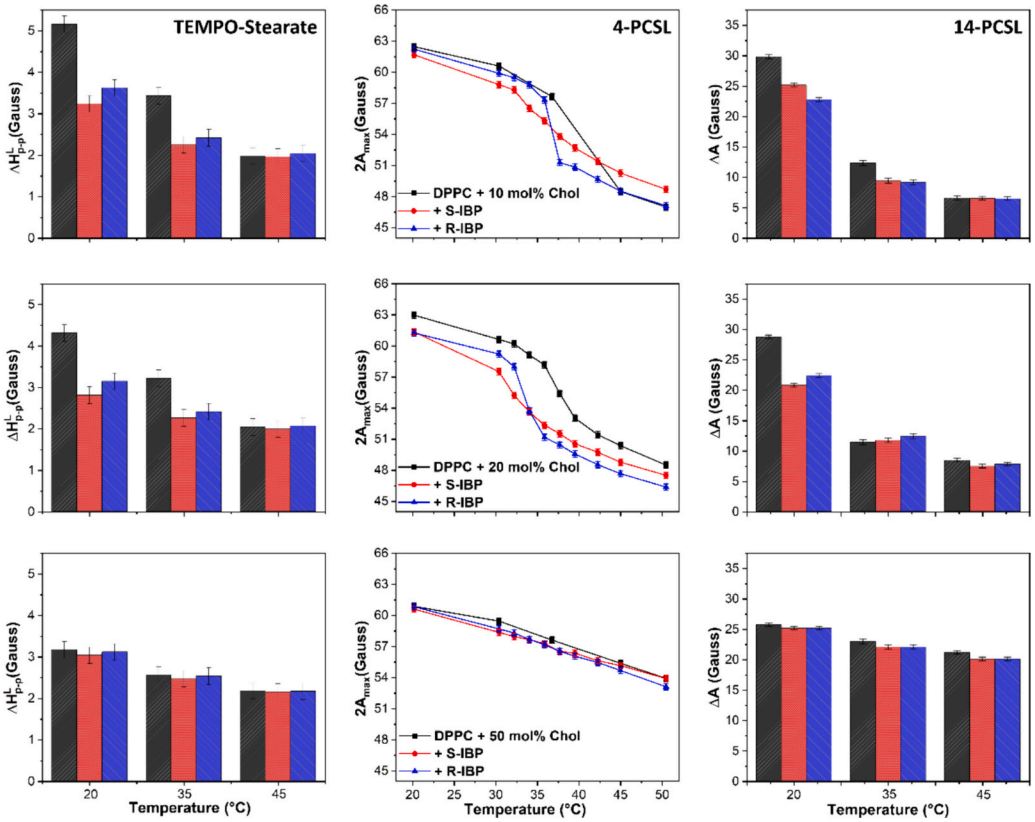

Fig. 5. Temperature dependence of ΔH^L_{p-p} of TEMPO-Stearate, $2A_{max}$ of 4-PCSL, and ΔA of 14-PCSL in bilayer mixtures of DPPC+10 mol% Chol (upper row), DPPC+20 mol% Chol (central row), and DPPC+50 mol% Chol (lower row) in the absence (black) and in the presence of 20 mol% of S-IBP (red) or R-IBP (blue).

and 50 mol%) on interaction of IBP in DPPC bilayers [23]. However, at variance with what observed in pure DPPC, our ESR data clearly indicate that cholesterol triggers a temperature-modulated enantiospecificity of IBP. In fact, from the data of TEMPO-Stearate and 14-PCSL for the samples DPPC +10 mol% Chol and DPPC+20 mol% Chol in Fig. 5 is evident an isomer-dependent membrane perturbation for temperature in the $S_o + L_o$ phase, i.e., at 20 and 35 °C, that is negligible in the liquid state, i.e., at 45 °C. Notably, in the same samples, the data of 4-PCSL indicate that the IBP chiral forms differently and considerably perturb the membranes at any temperature. The augmented perturbation of the IBP enantiomers at the first acyl chain segments probed by 4-PCSL could be due to the fact that this membrane region is close to the carbonyl CO groups and to the chiral lipid center, which are fundamental for the interaction between ester-linked diacyl-lipids and chiral molecules [16]. Another important aspect that can be singled out from Fig. 5 is that any temperature-mediated influence of IBP enantiomers is within the experimental uncertainty in the liquid-ordered membranes of DPPC and 50 mol% of cholesterol. In these samples, almost superimposable values of ΔH^L_{p-p}, $2A_{max}$ and ΔA are reported in the absence and in the presence of R- or S-IBP. Although the CD data in Fig. 1 indicate a separation parameter >1, it is likely that the low amount of IBP adsorbed on bilayers makes the membrane perturbation difficult to be detected.

Our study also sheds light on the positioning of IBP within cholesterol-containing PC bilayers, which is another topic widely discussed in literature [22–24,26,29,30]. Our ESR data of site-specific labelled lipids suggest that the amphiphilic IBP drug, upon interacting with DPPC bilayers, locates at the polar/apolar interface and penetrates the hydrocarbon region of the membrane. In the presence of 10 and 20 mol% Chol, IBP induces more perturbation on the polar-head and at the first chain segments than in the deep hydrocarbon interior. It is therefore likely that Chol displaces IBP to positions in the upper chain segments and close to the DPPC membrane surface. Literature discussions support these observations, reporting that in the presence of 20 mol% cholesterol, IBP (5 mol%) tends to be expelled from the membrane core and resides solely in the head group region [24]. A concentration-dependent distribution of IBP in the hydrocarbon region of phosphocholine membrane and a more superficial localization in a region closer to the head group of cholesterol-containing bilayers have been recently reported by Dzuba and coworkers [30]. Finally, our overall results suggest that the drug isoforms do not penetrate the hydrocarbon region and possible locate on the polar surface in DPPC bilayers containing 50 mol% of cholesterol.

3.3. *Atomic force microscopy: IBP induces enantiospecific morphological changes in mixtures of DPPC with 10 and 20 mol% Chol*

To delve deeper into the interaction between IBP isoforms and cholesterol-containing model membranes, and to underscore potential enantiospecific effects, AFM measurements were conducted on DPPC monolayers with varying cholesterol content (0, 10, 20, and 50 mol%) both in the absence and presence of S- or R-IBP, at the fixed concentration of 20 mol%. The resulting topographies of these films, deposited on mica surfaces at a constant pressure of 20 mN/m with dimensions of $2 \times 2\ \mu m^2$, are illustrated in Fig. 6.

The AFM image of pure DPPC monolayers (Fig. 6a) is characterized by extensive homogeneous regions, the bright ones, interspersed by dark regions, as also reported in [47,48], consistent with lipid molecules in the liquid condensed state. The addition of both S- and R-IPB to pure DPPC matrix does not alter the membrane surface morphology, which still exhibits homogeneous regions interspersed by dark ones (Fig. 6d and Fig. 6g, respectively). It is noteworthy that in the DPPC/S-IBP monolayers, some aggregates (i.e. white spots) are observed, which are likely due to an excess of IBP not fully incorporated into the DPPC matrix, i.e. preferentially located at the terminal methyl ends.

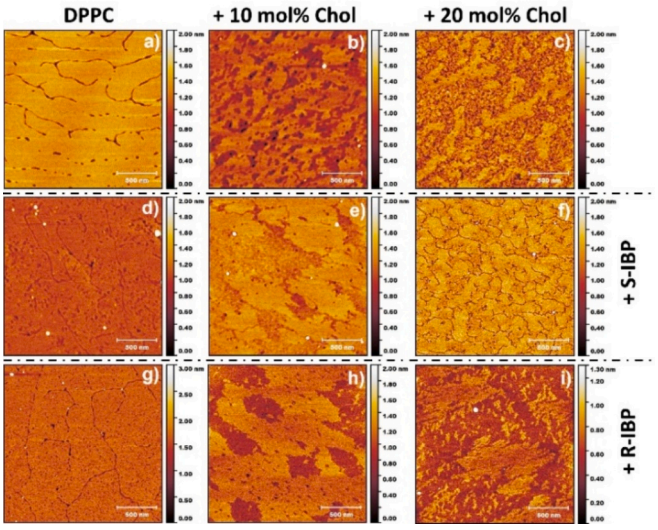

Fig. 6. AFM topography of Langmuir films deposited onto freshly cleaved mica at a pressure of 20 mN/m of a) DPPC; b) DPPC+10 mol% Chol; c) DPPC+ 20 mol% Chol; d) DPPC+20 mol% S-IBP; e) (DPPC+10 mol% Chol) + 20 mol% S-IBP, f) (DPPC+ 20 mol% Chol) + 20 mol% S-IBP; g) DPPC+20 mol% R-IBP; h) (DPPC+10 mol% Chol) + 20 mol% R-IBP; i) (DPPC+20 mol% Chol) + 20 mol% R-IBP. The scale bar is 500 nm.

Comparing the roughness, R_q, and height difference of the regions between pure DPPC and DPPC/S-IBP films, we noted an increased membrane roughness for the latter ($R_q = 0.17 \pm 0.02$ nm versus $R_q = 0.11 \pm 0.01$ nm), indicative of the presence of aggregates, and a slightly reduced height difference in the two regions (0.35 ± 0.20 nm versus 0.60 ± 0.30 nm). The DPPC/R-IBP monolayer (Fig. 6g) exhibits a well-defined structure compared to the DPPC/S-IBP one (Fig. 6d), owing a roughness similar to pure DPPC.

The observations on the morphology of DPPC monolayers in the absence and presence of IBP isomers further support the absence of enantiospecific effects of the drug on DPPC, demonstrating that S-IBP and its antipode incorporate into DPPC without substantially altering the film morphology (i.e., not perturbing the membrane structure), in close agreement with the spectroscopic data presented above.

The addition of 10, 20, and 50 % molar amounts of cholesterol to DPPC modifies the monolayer morphology. The surface morphology of DPPC+10 mol% Chol monolayer (Fig. 6b) shows holes-like structures, as a result of the low Chol amount addition, whereas that of DPPC+20 mol % Chol is characterized by condensed domains interspersed with holes (Fig. 6c). These features in the morphology are not surprising. In fact, they indicate the coexistence of two different phases, likely ascribed to the solid-order (cholesterol-poor) and liquid-ordered (cholesterol-rich) domains induced at low temperature in DPPC by Chol content in the range 10–30 mol% [49,50]. The addition of a equimolar content of Chol (i.e. DPPC +50 mol% Chol), produces homogenous monolayers almost free of defects (Fig. S 4a) due to the formation of compact layers in the liquid-ordered L_o phase. Similar features on membrane morphology changes due to the addition of Chol were previously reported on DPPC bilayers by [51].

The addition of IBP chiral forms into DPPC/Chol matrices reveals intriguing distinctions in their impact on film morphologies that are dependent on cholesterol content. Indeed, IBP enantiomers differently affect the topography at Chol concentration of 10 and 20 mol%. In contrast, minimal effects, i.e. the presence of few aggregates, are exhibited at 50 mol% Chol (see, Fig. S 4b and S 4c).

The (DPPC+10 mol% Chol) + S-IBP monolayer (Fig. 6e) showcases a morphology characterized by extensive areas of condensed domains alongside a few IBP aggregates, starkly different from the DPPC+10 mol % Chol surface structure. Consistent with the ESR findings mentioned in paragraph 3.2.2, the inclusion of S-IBP in cholesterol-doped DPPC membranes amplifies molecular disorder, resulting in distinct molecular packing reflected in the monolayer morphology. The introduction of R-IBP in DPPC+10 mol% Chol monolayer contributes to a clearer definition of the condensed domain areas observed for S-IBP, increasing the height disparity between them (0.75 ± 0.35 nm versus 0.35 ± 0.20 nm), showing a membrane surface lacking of aggregates (see Fig. 6h).

A notable dissimilarity in the interaction of the two IBP isomers is evident in the DPPC+20 mol% Chol monolayer. While the monolayer containing S-IBP presents a uniform surface interspersed by short interstices nearly devoid of aggregates (Fig. 6f), the one containing R-IBP is characterized by the presence of large domains surrounded by smaller ones, with a measured height difference of (0.53 ± 0.23 nm) and few aggregates (Fig. 6i).

Overall, from the AFM analysis conducted on both pure DPPC and DPPC/Chol monolayers exposed to IPB isomers, it can be concluded that the presence of 10–20 mol% of cholesterol facilitates the incorporation of IBP into the phospholipid matrices and, even more interestingly, induces enantioselective perturbations manifested on the membrane morphology.

4. Conclusions

A synergistic combination of different biophysics techniques, such as CD, spin-label ESR, and AFM, was employed to unravel the interaction between biomimetic membranes and drug enantiomers. It has been reported that enantiospecific effects of drugs on model membranes are triggered by a number of membrane properties, such as composition, fluidity, and structural heterogeneity. Our study focused on the effects of chiral forms of IBP (at the concentration of 20 mol%) on cholesterol-containing DPPC membranes (at 0, 10, 20, and 50 mol%). The results clearly show that the addition of cholesterol to DPPC is fundamental to elicit chiral-specific IBP effects. Moreover, they indicate that the enantiospecific effects are modulated by temperature and Chol concentration, i.e., parameters that determine the membrane physical state. The results can be summarized as follow. In pure DPPC, S- and R-IBP equally adsorb on DPPC bilayers, induce disorder across the bilayers, and downshift the main transition temperature. In mixtures of DPPC with 10 and 20 mol% Chol, S- and R- IBP differently absorb on membranes and enantiospecifically affect membrane properties. In particular, the ESR data indicate that, compared with the reference matrix, the IBP isomers differently loosen the molecular packing, especially in the $S_o + L_o$ state (at 20 and 35 °C) and negligibly in the ($L_d + L_o$) state (at 45 °C); this effect is more evident in the upper membrane region than at the bilayer midplane. Relevant are the unprecedented AFM results on the enantiospecific effects on film morphologies. In fact, in agreement with the spectroscopic data, AFM measurements also evidence distinct effects of IBP enantiomers in the morphological features of cholesterol-containing DPPC monolayers at 10 and, particularly, at 20 mol% Chol. Both the spectroscopic and the microscopic results indicate that the enantioselective perturbation of IBP within cholesterol-containing DPPC bilayers is markedly reduced at equimolar content, in the liquid-order L_o phase. The present experimental results on how the presence of cholesterol modulates the temperature-dependent enantiospecificity of IBP isomers in DPPC membrane model systems extend and complement the previous results obtained using only racemic IBP [23,26,29,30].

The results of our study contribute to the understanding of the intricate interplay between membrane composition and drug effects and highlight the importance of cholesterol in determining enantiospecificity of drugs in interaction with membranes.

CRediT authorship contribution statement

Alexa Guglielmelli: Writing – original draft, Validation, Methodology, Investigation, Conceptualization. **Caterina M. Tone:** Writing – original draft, Validation, Methodology, Investigation,

Conceptualization. **Eleonora Ragozzino:** Validation, Investigation. **Federica Ciuchi:** Writing – original draft, Validation, Methodology, Conceptualization. **Rosa Bartucci:** Writing – review & editing, Writing – original draft, Validation, Supervision, Conceptualization.

Declaration of competing interest

The authors declare that they have no known competing financial interests or personal relationships that could have appeared to influence the work reported in this paper.

Acknowledgements

A.G. acknowledges financial support from the "NLHT- Nanoscience Laboratory for Human Technologies" - (POR Calabria FESR-FSE 14/20 – CUP: J22C14000230007) and POS RADIOAMICA, project funded by the Italian Minister of Health (CUP: H53C22000650006). C.M.T. acknowledges PON "Attraction and International Mobility" R&I 2014−2020, AIM 1875705-2, CUP H24119000450005 and PON "Ricerca e Innovazione" 2014-2020, CUP H25F21001220006.

Appendix A. Supplementary data

Supplementary data to this article can be found online at https://doi.org/10.1016/j.bbamem.2024.184334.

References

[1] C. Peetla, A. Stine, V. Labhasetwar, Biophysical interactions with model lipid membranes: applications in drug discovery and drug delivery, Mol. Pharm. 6 (5) (2009) 1264–1276.
[2] L.M. Lichtenberger, Y. Zhou, V. Jayaraman, J.R. Doyen, R.G. O'Neil, E.J. Dial, R. Krishnamoorti, Insight into NSAID-induced membrane alterations, pathogenesis and therapeutics: characterization of interaction of NSAIDs with phosphatidylcholine, Biochim. Biophys. Acta-Molec. Cell Biol. Lipids 1821 (7) (2012) 994–1002.
[3] C. Pereira-Leite, C. Nunes, S. Reis, Interaction of nonsteroidal anti-inflammatory drugs with membranes: in vitro assessment and relevance for their biological actions, Prog. Lipid Res. 52 (4) (2013) 571–584.
[4] H. Tsuchiya, Stereospecificity in membrane effects of catechins, Chem. Biol. Interact. 134 (1) (2001) 41–54.
[5] M. Mizogami, H. Tsuchiya, T. Ueno, M. Kashimata, K. Takakura, Stereospecific interaction of bupivacaine enantiomers with lipid membranes, Reg. Anesth. Pain Med. 33 (4) (2008) 304–311.
[6] H. Tsuchiya, M. Mizogami, The membrane interaction of drugs as one of mechanisms for their enantioselective effects, Med. Hypotheses 79 (1) (2012) 65–67.
[7] P. Gusain, S. Ohki, K. Hoshino, Y. Tsujino, N. Shimokawa, M. Takagi, Chirality-dependent interaction of D-and L-menthol with biomembrane models, Membranes 7 (4) (2017) 69.
[8] H.S. Martin, K.A. Podolsky, N.K. Devaraj, Probing the role of chirality in phospholipid membranes, ChemBioChem 22 (22) (2021) 3148–3157.
[9] A.V. Mastova, O.Y. Selyutina, N.E. Polyakov, Stereoselectivity of interaction of nonsteroidal anti-inflammatory drug S-Ketoprofen with L/D-tryptophan in phospholipid membranes, Membranes 12 (5) (2022) 460.
[10] A. Guglielmelli, G. Palermo, G. Strangi, Unveiling chirality: exploring nature's blueprint for engineering plasmonic materials, MRS Commun. 13 (5) (2023) 704–713.
[11] A. Lininger, G. Palermo, A. Guglielmelli, G. Nicoletta, M. Goel, M. Hinczewski, G. Strangi, Chirality in light–matter interaction, Adv. Mater. 35 (34) (2023) 2107325.
[12] P. Novotná, F. Králík, M. Urbanová, Chiral recognition of bilirubin and biliverdin in liposomes and micelles, Biophys. Chem. 205 (2015) 41–50.
[13] T. Ishigami, K. Suga, H. Umakoshi, Chiral recognition of L-amino acids on liposomes prepared with L-phospholipid, ACS Appl. Mater. Interfaces 7 (38) (2015) 21065–21072.
[14] T. Ishigami, A. Tauchi, K. Suga, H. Umakoshi, Effect of boundary edge in DOPC/DPPC/cholesterol liposomes on acceleration of l-histidine preferential adsorption, Langmuir 32 (24) (2016) 6011–6019.
[15] Y. Okamoto, Y. Kishi, T. Ishigami, K. Suga, H. Umakoshi, Chiral selective adsorption of ibuprofen on a liposome membrane, J. Phys. Chem. B 120 (10) (2016) 2790–2795.
[16] A. Guglielmelli, R. Bartucci, B. Rizzuti, G. Palermo, R. Guzzi, G. Strangi, The interaction of tryptophan enantiomers with model membranes is modulated by polar head type and physical state of phospholipids, Colloids Surf. B: Biointerfaces 224 (2023) 113216.
[17] A.M. Evans, Comparative pharmacology of S (+)-ibuprofen and (RS)-ibuprofen, Clin. Rheumatol. 20 (2001) 9–14.
[18] G. Van Meer, D.R. Voelker, G.W. Feigenson, Membrane lipids: where they are and how they behave, Nat. Rev. Mol. Cell Biol. 9 (2) (2008) 112–124.
[19] J. Lombard, P. López-García, D. Moreira, The early evolution of lipid membranes and the three domains of life, Nat. Rev. Microbiol. 10 (7) (2012) 507–515.
[20] M. Manrique-Moreno, P. Garidel, M. Suwalsky, J. Howe, K. Brandenburg, The membrane-activity of ibuprofen, diclofenac, and naproxen: a physico-chemical study with lecithin phospholipids, Biochim. Biophys. Acta-Biomembr. 1788 (6) (2009) 1296–1303.
[21] M.B. Boggara, R. Krishnamoorti, Small-angle neutron scattering studies of phospholipid-NSAID adducts, Langmuir 26 (8) (2010) 5734–5745.
[22] M.B. Boggara, M. Mihailescu, R. Krishnamoorti, Structural association of nonsteroidal anti-inflammatory drugs with lipid membranes, J. Am. Chem. Soc. 134 (48) (2012) 19669–19676.
[23] A. Khajeh, H. Modarress, The influence of cholesterol on interactions and dynamics of ibuprofen in a lipid bilayer, Biochim. Biophys. Acta-Biomembr. 1838 (10) (2014) 2431–2438.
[24] R.J. Alsop, C.L. Armstrong, A. Maqbool, L. Toppozini, H. Dies, M.C. Rheinstädter, Cholesterol expels ibuprofen from the hydrophobic membrane core and stabilizes lamellar phases in lipid membranes containing ibuprofen, Soft Matter 11 (24) (2015) 4756–4767.
[25] M. Di Foggia, S. Bonora, A. Tinti, V. Tugnoli, DSC and Raman study of DMPC liposomes in presence of Ibuprofen at different pH, J. Therm. Anal. Calorim. 127 (2017) 1407–1417.
[26] S.L. Yefimova, T.N. Tkacheva, N.A. Kasian, Study of the combined effect of ibuprofen and cholesterol on the microviscosity and ordering of model lipid membranes by time resolved measurement of fluorescence anisotropy decay, J. Appl. Spectrosc. 84 (2017) 284–290.
[27] E. Aloi, B. Rizzuti, R. Guzzi, R. Bartucci, Association of ibuprofen at the polar/apolar interface of lipid membranes, Arch. Biochem. Biophys. 654 (2018) 77–84.
[28] V.K. Sharma, M. Nagao, D.K. Rai, E. Mamontov, Membrane softening by nonsteroidal anti-inflammatory drugs investigated by neutron spin echo, Phys. Chem. Chem. Phys. 21 (2019) 20211.
[29] J. Kremkow, M. Luck, D. Huster, P. Müller, H.A. Scheidt, Membrane interaction of ibuprofen with cholesterol-containing lipid membranes, Biomolecules 10 (10) (2020) 1384.
[30] A.S. Kashnik, O.Y. Selyutina, D.S. Baranov, N.E. Polyakov, S.A. Dzuba, Localization of the ibuprofen molecule in model lipid membranes revealed by spin-label-enhanced NMR relaxation, Biochim. Biophys. Acta-Biomembr. 1865 (8) (2023) 184215.
[31] D. Marsh, Liquid-ordered phases induced by cholesterol: a compendium of binary phase diagrams, Biochim. Biophys. Acta-Biomembr. 1798 (3) (2010) 688–699.
[32] D. Marsh, Handbook of Lipid Bilayers, CRC press, 2013.
[33] M.O. Okuom, R. Burks, C. Naylor, A.E. Holmes, Applied circular dichroism: a facile spectroscopic tool for configurational assignment and determination of enantiopurity, J. Anal. Methods Chem. (2015) 2015.
[34] D. Marsh, A. Watts, in: P.C. Jost, O.H. Griffith (Eds.), Lipid–Protein Interactions vol. 2, Wiley Interscience, New York, 1982, pp. 53–126.
[35] D.D. Lasic, Liposomes: From Physics to Applications, Elsevier Science, 1993.
[36] E. Aloi, R. Bartucci, Interdigitated lamellar phases in the frozen state: spin-label CW-and FT-EPR, Biophys. Chem. 253 (2019) 106229.
[37] E. Aloi, C.M. Tone, R.C. Barberi, F. Ciuchi, R. Bartucci, Effects of curcumin in the interaction with cardiolipin-containing lipid monolayers and bilayers, Biophys. Chem. 301 (2023) 107082.
[38] A. Rodger, B. Nordén, Circular Dichroism and Linear Dichroism vol. 1, Oxford University Press, USA, 1997.
[39] D. Nečas, P. Klapetek, Gwyddion: an open-source software for SPM data analysis, Open Phys. 10 (1) (2012) 181–188.
[40] S. Jullien, A. Vertut-Croquin, J. Brajtburg, J. Bolard, Circular dichroism for the determination of amphotericin B binding to liposomes, Anal. Biochem. 172 (1) (1988) 197–202.
[41] D. Marsh, Electron spin resonance: spin labels, Membr. Spectr. (1981) 51–142.
[42] D. Marsh, Spin-label electron paramagnetic resonance spectroscopy, CRC Press, 2019.
[43] R. Bartucci, T.L. Pali, D. Marsh, Lipid chain motion in an interdigitated gel phase: conventional and saturation transfer ESR of spin-labeled lipids in dipalmitoylphosphatidylcholine-glycerol dispersions, Biochemistry 32 (1993) 274–281.
[44] K. Simons, E. Ikonen, Functional rafts in cell membranes, Nature 387 (6633) (1997) 569–572.
[45] A. Radhakrishnan, H.M. McConnell, Cholesterol-phospholipid complexes in membranes, J. Am. Chem. Soc. 121 (2) (1999) 486–487.
[46] K. Simons, D. Toomre, Lipid rafts and signal transduction, Nat. Rev. Mol. Cell Biol. 1 (1) (2000) 31–39.
[47] L.K. Nielsen, A. Vishnyakov, K. Jørgensen, T. Bjørnholm, O.G. Mouritsen, Nanometre-scale structure of fluid lipid membranes, J. Phys. Condens. Matter 12 (8A) (2000) A309.
[48] K.H. Kim, S.Q. Choi, Z.A. Zell, T.M. Squires, J.A. Zasadzinski, Effect of cholesterol nanodomains on monolayer morphology and dynamics, Proc. Natl. Acad. Sci. U. S. A. (2013) E3054–E3060.

[49] M.B. Sankaram, T.E. Thompson, Interaction of cholesterol with various glycerophospholipids and sphingomyelin, Biochemistry 29 (1990) 10670–10675.
[50] M.B. Sankaram, T.E. Thompson, Cholesterol-induced fluid-phase immiscibility in membranes, Proc. Natl. Acad. Sci. U. S. A. 88 (1991) 8686–8690.
[51] L. Redondo-Morata, M.I. Giannotti, F. Sanz, Influence of cholesterol on the phase transition of lipid bilayers: a temperature-controlled force spectroscopy study, Langmuir 28 (35) (2012) 12851–12860.